Received: 28 June 2022 | Revised: 15 July 2022 | Accepted: 15 July 2022

DOI: 10.1111/jace.18686

Journal of the American Ceramic Society

RAPID COMMUNICATION

Microstructure and conductivity of blacklight-sintered TiO_2, YSZ, and $Li_{0.33}La_{0.57}TiO_3$

Lukas Porz[1] | **Michael Scherer**[1] | **Qaisar Khushi Muhammad**[1] | **Kimitaka Higuchi**[2] | **Yan Li**[3] | **Shuhei Koga**[3] | **Atsutomo Nakamura**[3] | **Wolfgang Rheinheimer**[4] | **Till Frömling**[1]

[1]Department of Materials and Earth Sciences, Technical University of Darmstadt, Darmstadt, Germany

[2]Institute of Materials and Systems for Sustainability, Nagoya University, Nagoya, Japan

[3]Department of Mechanical Science and Bioengineering, Osaka University, Osaka, Japan

[4]Forschungszentrum Jülich GmbH, Institute for Energy and Climate Research, Jülich, Germany

Correspondence
Lukas Porz, Department of Materials and Earth Sciences, Technical University of Darmstadt, Darmstadt, Germany.
Email: porz@ceramics.tu-darmstadt.de

Funding information
Deutsche Forschungsgemeinschaft, Grant/Award Numbers: 414179371, RH146/1-1; Bundesministerium für Bildung und Forschung, Grant/Award Number: 03XP0146; JST PRESTO, Grant/Award Number: JPMJPR199A; JSPS KAKENHI, Grant/Award Numbers: JP21H04532, JP19H05786

Abstract

Rapid densification of ceramics has been realized and its merits were demonstrated through multiple approaches out of which UHS and flash sintering attract recent attention. So far, however, scalability remains difficult. A rise in throughput and scalability is enabled by the introduction of blacklight sintering powered by novel light source technology. Intense illumination with photon energy above the bandgap (blacklight) allows high absorption efficiency and, hence, very rapid, contactless heating for all ceramics. While heating the ceramic directly with light without any furnace promises scalability, it simultaneously offers highly accurate process control. For the technology transfer to industry, attainable material quality needs to be assured. Here, we demonstrate the excellent microstructure quality of blacklight-sintered ceramics observed with ultrahigh voltage electron microscopy revealing an option to tune nanoporosity. Moreover, we confirm that electronic, electron, oxygen, and lithium-ion conductivities are equal to conventionally sintered ceramics. This gives the prospect of transmitting the merits of rapid densification to the scale of industrial kilns.

KEYWORDS
blacklight sintering, conductivity, microstructure, sinter/sintering

1 | INTRODUCTION

Rapid sintering of ceramics attracted recent attention for accelerated compositional development and increased process speed.[1,2] Spark plasma sintering with a heated die,[3] flash sintering with an electric current through the samples,[4–6] and ultrafast high-temperature sintering (UHS) with samples in intimate contact with heated carbon tapes,[1,7] as well as microwave sintering,[8] have already demonstrated rapid sintering and its merits. To

compete with conventional sintering,[9] such fast processing approaches must become more practical and industrially scalable.

Blacklight as a power transmitting medium is suggested to be a very straightforward approach to realizing rapid sintering.[10] Green bodies are heated within seconds merely through intense illumination with photon energies above the bandgap, allowing a contactless and containerless process. This minimizes process and sample change times, opening the door to immediate industrial scaling. Moreover, it holds the potential to beat the energy efficiency of industrial-scale furnaces independent of batch size while replacing natural gas with intermittently available renewable electricity.[10–12]

Rapid sintering can alter the defect structure within the produced ceramics. The modified defect chemistry ultimately translates to an impact of the processing technique on the behavior of the final material. Alongside the high heating and cooling rates,[13] electric fields within the ceramic and/or reducing atmosphere are key contributors to defect creation in established rapid sintering techniques.[14] Avoiding currents in the sample or a reducing atmosphere will allow more control over the densification process and material properties. Therefore, blacklight sintering has great potential to provide material qualities that match or even exceed large-scale furnace sintering.

Here, electronically conducting TiO_2, oxygen ion conducting YSZ, and Li-ion conducting $Li_{0.33}La_{0.57}TiO_3$ are chosen as model materials to study the impact of blacklight sintering,[10] on the electrical conductivity. The ceramics are characterized in detail with XRD and ultrahigh voltage electron microscopy (UHVEM). The electrical conductivity is reported for all three materials and compared to conventionally sintered references. Moreover, all results are cross-validated using blacklight sintering with a 450-nm laser and an Xe-flash lamp.

2 | EXPERIMENTAL PROCEDURES

Synthesis of the blacklight-sintered samples is described in great detail in an accompanying publication.[10] A Xe-flash lamp pulsed at 60 Hz was used in the test labs of Heraeus Noblelight, Cambridge, UK, whereas a 450-nm laser was used in the test labs of Laserline, Mülheim-Kärlich, Germany. TiO_2 was sintered on ceramic wool insulation, whereas YSZ and $Li_{0.33}La_{0.57}TiO_3$ were sintered on expandable graphite. Parameters were reported in Table 1, temperature curves in Figure 5, and SEM micrographs in supplementary materials 9 and 10 of the accompanying publication.[10]

Electrical conductivity data was recorded with impedance spectroscopy using an impedance analyzer (Novocontrol, Montabaur, Germany). Temperature-dependent conductivity was recorded during cooling after a 2-h holding time at 800°C. Oxygen partial pressure (pO_2)-dependent data was recorded in the range of 10^{-1}–10^{-5} bar at 700°C after 40 min of holding time for each data point. Such procedure, the temperature range, and the rationale behind it were established elsewhere.[15]

Electrodes from Pt-paste fired at 930°C for 5 min were used for all measurements. No sample post-processing after blacklight sintering, such as grinding off surfaces, was required. UHVEM samples were thinned by conventional polishing and ion milling (Fischione Model 1051). The acceleration voltage was set to 1 MV in TEM or STEM mode using the JEOL JEM-1000k RS at Nagoya University. Here, the UHVEM is used to better analyze internal structures with various types of pores in the samples.

3 | RESULTS AND DISCUSSION

Produced densities were beyond 99% for $Li_{0.33}La_{0.57}TiO_3$, 94%–98% for TiO_2, and 87% for YSZ. The microstructure was found to be homogenous across the entire sample thickness with next to no cracks observed; see also supplementary materials 4, 9, and 10 elsewhere.[10] Here, UHVEM reveals the microstructure and pore distribution in much greater detail.

Basically, no pores were observed in the >99% dense $Li_{0.33}La_{0.57}TiO_3$, as displayed in Figure 1C. This shows that rapid densification with blacklight is capable of producing high densities approaching 100%. In contrast, connected pores in the 87% dense YSZ (see Figure 1D) hint toward incomplete sintering and too low process temperatures. Higher illumination power or a longer illumination application is needed for full densification. The respective sintering process of the ceramics depends on the bandgap and its temperature dependence, the related absorption efficiency, light exposure time, and even the properties of the substrate on which the ceramic is positioned.[10] This gives a wide range of optimization opportunities. For example, porosity or grain size gradients can be generated. Concerning the grain sizes, no significant differences from regularly sintered material were found for TiO_2 or YSZ samples in this work.[10,16] However, the $Li_{0.33}La_{0.57}TiO_3$ is not only denser but seems to exhibit grain sizes from the lower end of the spectrum.[17,18]

No significant difference is found when contrasting the microstructure on TEM images of TiO_2 synthesized with 450-nm laser and Xe-flash lamp in Figure 1A,B. This shows the generality of the approach and its applicability with different kinds of suitable light sources. The grain size was determined to be $5.8 \pm 0.6\ \mu m$ for samples produced with

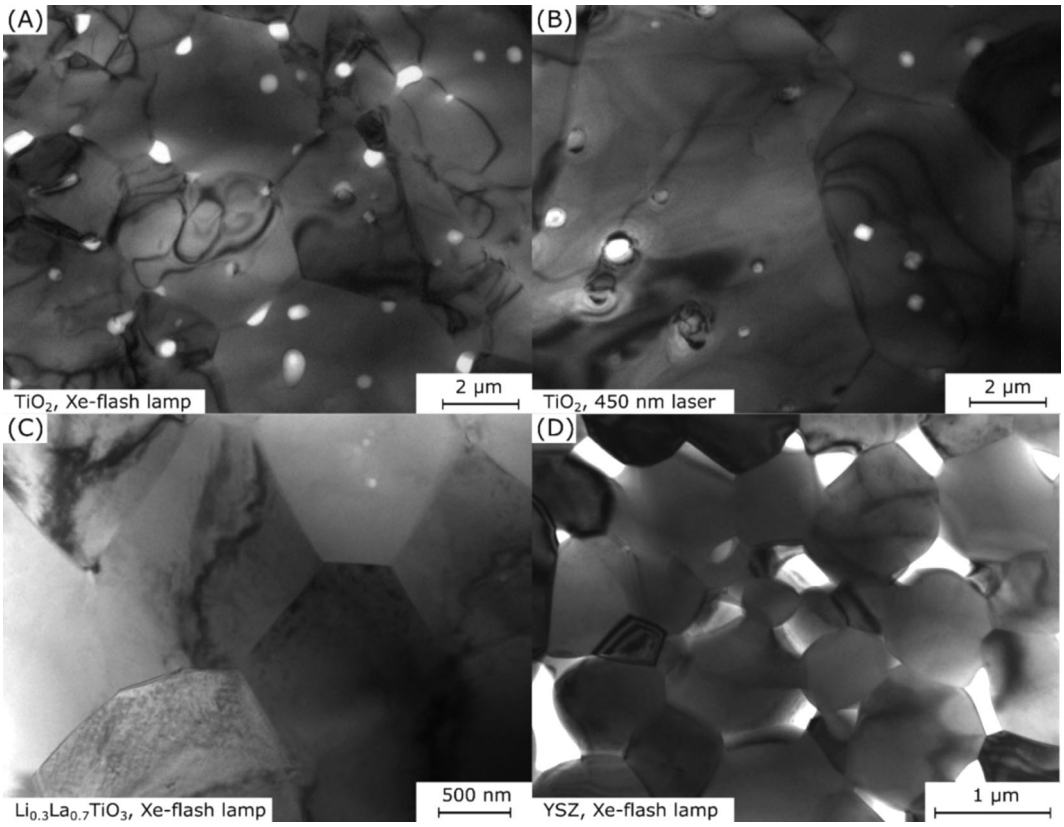

FIGURE 1 Ultrahigh voltage electron microscopy (UHVEM) analysis of blacklight-sintered ceramics. (A and B) Comparison of the microstructure of TiO_2 generated with an Xe-flash lamp and 450-nm laser illustrating negligible differences in synthesis outcome aside from the grain size. Pores with a diameter of below 1 μm are frequently observed in both cases, located either at grain boundaries or in the bulk of the grains. (C) Fully dense microstructure of $Li_{0.33}La_{0.57}TiO_3$. (D) YSZ after incomplete sintering

the 450-nm laser and 10.9 ± 1.1 μm for samples sintered with the Xe-flash lamp.

Moreover, UHVEM reveals nanopores at grain boundaries, within the grains, and on triple points of TiO_2. A pore density of 30 pores per 100 μm^2 with a pore diameter of 0.35 ± 0.13 μm was found for the sample sintered with a 450-nm laser. The majority of the pores were found inside grains with a fraction of 10%–15% at grain boundaries and another 10%–15% at triple points. A slightly lower pore density of eight pores per 100 μm^2 was found in the sample sintered using an Xe-flash lamp, however, with a comparable diameter of 0.38 ± 0.11 μm. Pore diameters are notably small with respect to the microstructure as they are significantly less than 1/10th of the grain size (refer to Figure 1B). Such porosities are very unusual for conventional sintering. However, similar porosity was found after UHS sintering.[19] Apparently, the sintering trajectories for high heating rates differ from conventional sintering.[20,21] To confirm proper synthesis, XRD patterns were recorded, as shown in Figure 2. No or negligible indications for secondary phases were observed, confirming a synthesis outcome at par with conventional sintering.

The electrical conductivities of TiO_2 of the conventionally sintered specimen and the ones produced with an Xe-flash lamp and a 450-nm laser are illustrated in Figure 3A. In the comparison, bulk conductivity and total conductivity, including grain boundary resistance, are separated. Taking the error bar of the measurements into account, the depicted values are very similar, which documents the negligible differences between synthesis methods. Additionally, oxygen partial pressure-dependent conductivity measurement conducted for a sample sintered with 450-nm laser reveals that the conductivity agrees well with what is expected for undoped TiO_2 and is in the conductivity minimum between electron and hole conductivity,[15,22,23] see Figure 3B. The nanoporosity observed in the microstructures appears not noteworthily affect the conductivity here.

Bulk conductivity for conventionally sintered YSZ and blacklight-sintered YSZ samples produced with 450-nm laser and Xe-flash lamp YSZ samples, again, lie within the error bar of the respective values, see Figure 3C. These are also in accordance with literature values.[24] The total conductivity of the blacklight-sintered materials is slightly lower than the reference, which is likely associated with

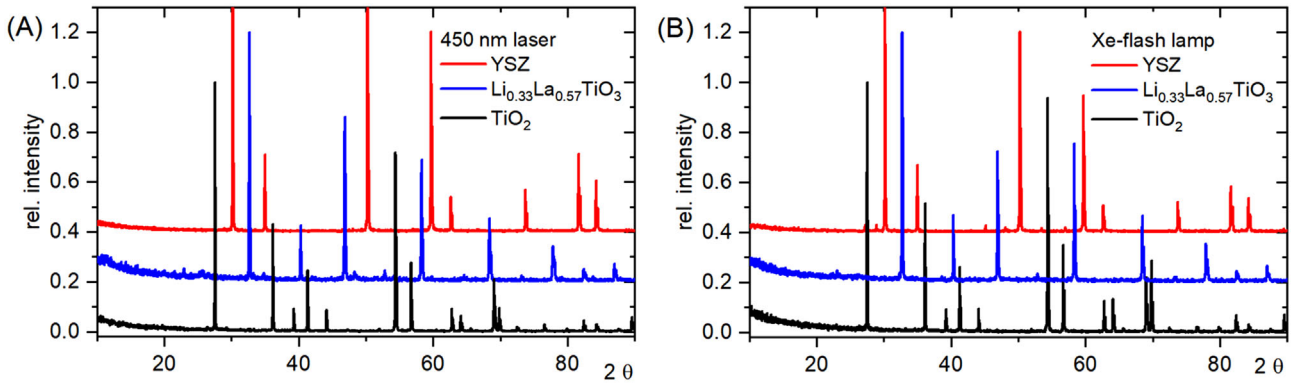

FIGURE 2 XRD patterns recorded for blacklight-sintered samples: (A) for samples synthesized with a 450-nm laser and (B) for samples synthesized with an Xe-flash-lamp

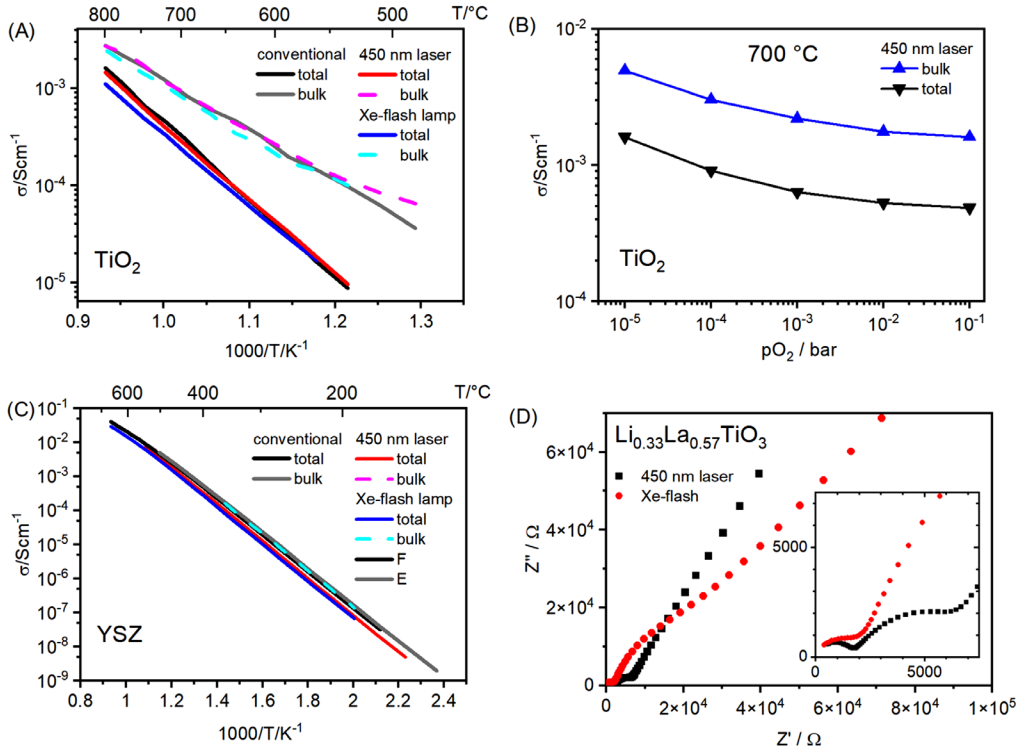

FIGURE 3 Conductivity of blacklight-sintered ceramics. (A) Temperature-dependent conductivity of TiO_2 comparing conventional sintering with fabrication with 450-nm laser and Xe-flash lamp. (B) Oxygen partial pressure-dependent conductivity of TiO_2 fabricated with a 450-nm laser illustrating its undoped states in the conductivity minimum. (C) Conductivity of 8-YSZ comparing conventional sintering with fabrication with 450-nm laser and Xe-flash lamp. (D) Impedance spectroscopy of $Li_{0.33}La_{0.57}TiO_3$ fabricated with Xe-flash lamp and 450-nm laser using a fired Pt electrode. Bulk resistance and interface resistance can be identified clearly, followed by a Warburg diffusion response.[17,28] The bulk resistivity of the laser fabricated sample is 0.15 mS/cm demonstrating an outstanding sintering outcome for this material.[17]

the low density.[25] As described in the previous work, the density and microstructure can be controlled, and a low density or gradient in density can also be beneficial for YSZ, for example, for sensor applications to obtain a high surface area.[10]

The impedance spectrum of the $Li_{0.33}La_{0.57}TiO_3$, produced with 450-nm laser and Xe-flash lamp, as shown in Figure 3D, reveals a bulk and grain boundary resistance and an electrode polarization tail at low frequencies. Resistances for the Xe-flash lamp–sintered samples

are higher than for the 450-nm laser in this case. The bulk conductivity of $Li_{0.33}La_{0.57}TiO_3$ produced with a 450-nm laser is 0.15 mS/cm, whereas the total conductivity is 4×10^{-4} S/cm. This is a high value for such a composition,[17,26,27] which illustrates its suitability for synthesizing battery materials. Moreover, we note the high density exceeding 99% and the strong control over the grain boundary conductivity enabled here, which are key parameters for the application of this battery material.[25]

4 | CONCLUSION

Synthesis results of blacklight sintering appear comparable to conventional sintering in all regards. The investigated benchmark ceramics TiO_2, YSZ, and LLTO all exhibit the same or similar electrical conductivity compared to regularly sintered reference material. UHVEM confirms defect-free microstructure aside from nanopores. Hence, blacklight sintering exploits all the merits of rapid sintering while producing excellent electrical properties for the electronically and ionically conductive materials. Its potential for upscaling and competitive energy efficiency makes it a very promising densification technique for the 21st century.

ACKNOWLEDGMENTS

Sabrina Kahse and Johannes Puy are acknowledged for sample pre- and post-processing. Martin Brown, Peter Lascelles, and Ross Kitson from Heraeus Noblelight are gratefully acknowledged for facilitating experimental capacities. We thank Daniel Huhn, Luisa-Marie Heine, and Simon Britten from Laserline for facilitating experimental capacities. Jürgen Rödel is acknowledged for helpful comments. We are thankful for funding form the Deutsche Forschungsgemeinschaft (DFG) under Grant no. 414179371 and RH 146/1-1 (W.R.). A.N. acknowledges the financial supports of JST PRESTO, Grant nos. JPMJPR199A and JSPS KAKENHI, JP21H04532 and JP19H05786, Japan. Till Frömling would like to thank the German Ministry of Education and Research (BMBF) for funding the program "NanoMatFutur" (Grant no. 03XP0146).

Open access funding enabled and organized by Projekt DEAL.

CONFLICT OF INTEREST

L.P., W.R., and M.S. have filed a patent application with the number PCT/EP2022/056389.

ORCID

Lukas Porz https://orcid.org/0000-0003-3163-085X
Michael Scherer https://orcid.org/0000-0002-4232-3399
Atsutomo Nakamura https://orcid.org/0000-0002-4324-1512
Wolfgang Rheinheimer https://orcid.org/0000-0002-2906-4265
Till Frömling https://orcid.org/0000-0002-8827-1926

REFERENCES

1. Wang C, Ping W, Bai Q, Cui H, Hensleigh R, Wang R, et al. A general method to synthesize and sinter bulk ceramics in seconds. Science. 2020;368(6490):521–6.
2. Harmer MP, Brook RJ. Fast firing – microstructural benefits. Br Ceram Trans J. 1981;80(5):147–8.
3. Munir ZA, Anselmi-Tamburini U, Ohyanagi M. The effect of electric field and pressure on the synthesis and consolidation of materials: a review of the spark plasma sintering method. J Mater Sci. 2006;41(3):763–77.
4. Raj R. Joule heating during flash-sintering. J Eur Ceram Soc. 2012;32(10):2293–301.
5. Cologna M, Rashkova B, Raj R. Flash sintering of nanograin zirconia in < 5 s at 850 degrees C. J Am Ceram Soc. 2010;93(11):3556–9.
6. Yu M, Grasso S, Mckinnon R, Saunders T, Reece MJ. Review of flash sintering: materials, mechanisms and modelling. Adv Appl Ceram. 2017;116(1):24–60.
7. Ihrig M, Mishra TP, Scheld WS, Häuschen G, Rheinheimer W, Bram M, et al. $Li_7La_3Zr_2O_{12}$ solid electrolyte sintered by the ultrafast high-temperature method. 2021;41:6075–9.
8. Rybakov KI, Olevsky EA, Krikun EV. Microwave sintering: fundamentals and modeling. J Am Ceram Soc. 2013;96(4):1003–20.
9. Bordia RK, Kang SJL, Olevsky EA. Current understanding and future research directions at the onset of the next century of sintering science and technology. J Am Ceram Soc. 2017;100(6):2314–52.
10. Porz L, Scherer M, Huhn D, Heine L-M, Britten S, Rebohle L, et al. Blacklight sintering of ceramics. Mater Horiz. 2022;9:1717–26.
11. Weber H. Use of hydrogen as fuel in kilns for the ceramics industry – are H_2 hybrid kilns being built. CFI/Ber DKG. 2022;99(1):E17–20.
12. Hajduk A. Clean and green: challenges and opportunities for industrial kiln construction in a post-COVID era. CFI/Ber DKG. 2022;99(2):E27–32.
13. Chu M-Y, Rahaman MN, De Jonghe LC, Brook RJ. Effect of heating rate on sintering and coarsening. J Am Ceram Soc. 1991;74(6):1217–25.
14. Guillon O, De Souza RA, Mishra TP, Rheinheimer W. Electric-field-assisted processing of ceramics: nonthermal effects and related mechanisms. MRS Bull. 2021;46(1):52–8.
15. Muhammad QK, Porz L, Nakamura A, Matsunaga K, Rohnke M, Janek J, et al. Self-doping by mechanically induced dislocations in bulk TiO_2. Nano Energy. 2021;85:105944.
16. Han M, Tang X, Yin H, Peng S. Fabrication, microstructure and properties of a YSZ electrolyte for SOFCs. J Power Sources. 2007;165(2):757–63.
17. Polczyk T, Zając W, Ziąbka M, Świerczek K. Mitigation of grain boundary resistance in $La_{2/3-x}Li3_xTiO_3$ perovskite as

an electrolyte for solid-state Li-ion batteries. J Mater Sci. 2021;56(3):2435–50.
18. Wolfenstine J, Allen JL, Read J, Sakamoto J, Gonalez-Doncel G. Hot-pressed $Li_{0.33}La_{0.57}TiO_3$. J Power Sources. 2010;195(13):4124–8.
19. Mishra TP, Wang S, Lenser C, Jennings D, Kindelmann M, Rheinheimer W, et al. Ultra-fast high-temperature sintering of strontium titanate. Acta Mater. 2022;231:117918.
20. German RM. Sintering trajectories: description on how density, surface area, and grain size change. JOM (US). 2016;68(3):878–84.
21. Shaw NJ Brook RJ. Structure and grain coarsening during the sintering of alumina. J Am Ceram Soc. 1986;69(2):107–10.
22. Bak T, Nowotny J, Rekas M, Sorrell CC. Defect chemistry and semiconducting properties of titanium dioxide: I. Intrinsic electronic equilibrium☆. J Phys Chem Solids. 2003;64(7):1043–56.
23. Nowotny J, Bak T, Burg T. Electrical properties of polycrystalline TiO_2 at elevated temperatures. Electrical conductivity. Phys Status Solidi B. 2007;244(6):2037–54.
24. Badwal SPS. Zirconia-based solid electrolytes: microstructure, stability and ionic conductivity. Solid State Ionics. 1992;52(1):23–32.
25. Vendrell X, Yadav D, Raj R, West AR. Influence of flash sintering on the ionic conductivity of 8 mol% yttria stabilized zirconia. J Eur Ceram Soc. 2019;39(4):1352–58.
26. Knauth P. Inorganic solid Li ion conductors: an overview. Solid State Ionics. 2009;180(14–16) 911–16.
27. Zheng F, Kotobuki M, Song SF, Lai MO, Lu L. Review on solid electrolytes for all-solid-state lithium-ion batteries. J Power Sources. 2018;389:198–213.
28. Criado C, Galán-Montenegro P, Velásquez P, Ramos-Barrado JR. Diffusion with general boundary conditions in electrochemical systems. J Electroanal Chem. 2000;488(1):59–63.

How to cite this article: Porz L, Scherer M, Muhammad QK, Higuchi K, Li Y, Koga S, et al. Microstructure and conductivity of blacklight-sintered TiO_2, YSZ, and $Li_{0.33}La_{0.57}TiO_3$. J Am Ceram Soc. 2022;105:7030–7035. https://doi.org/10.1111/jace.18686